

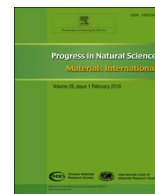
HOSTED BY



ELSEVIER

Contents lists available at ScienceDirect

Progress in Natural Science: Materials International

journal homepage: www.elsevier.com/locate/pnsmi

Original Research

Characterization of $\text{Bi}_{2/3}\text{Cu}_3\text{Ti}_4\text{O}_{12}$ ceramics synthesized by semi-wet routePooja Gautam^a, Ankur Khare^a, Sunita Sharma^a, N.B. Singh^b, K.D. Mandal^{a,*}^a Department of Chemistry, Indian Institute of Technology (BHU), Varanasi-221005, U.P, India^b Department of Chemistry & Biochemistry, University of Maryland, Baltimore County, 1000 Hilltop Circle, Baltimore, MD 21250, USA

ARTICLE INFO

Keywords:

Ceramic
Synthesis
Structural properties
Magnetic properties

ABSTRACT

$\text{Bi}_{2/3}\text{Cu}_3\text{Ti}_4\text{O}_{12}$ (BCTO) ceramic was synthesized by the semi-wet route using metal nitrate solutions and solid TiO_2 powder in a stoichiometric ratio. Fourier transform infrared (FTIR) study of BCTO precursor powder and calcined ceramic showed the presence of alcoholic functional groups and the stretching band of Ti-O and Cu-O respectively. X-ray diffraction (XRD), scanning electron microscope (SEM) and energy dispersive x-ray spectroscopy (EDX) were employed to characterize the structure, surface morphology and purity of the sintered BCTO ceramic respectively. X-ray diffraction study confirmed the single phase formation of BCTO ceramic at 1073 K. The average dimension of grains calculated by SEM and AFM was found to be in the range of $0.73 \pm 0.2 \mu\text{m}$ with clear grain boundaries. Magnetic property was investigated over a wide temperature range 2–300 K at a magnetic field of 7 tesla. The Curie temperature was calculated by zero field cooled (M^{ZFC}) and field cooled (M^{FC}) magnetization at 100 Oe applied field which was found to be 125 K. The sintered BCTO ceramic shows high dielectric constant ($\epsilon' = 2.9 \times 10^4$) at 323 K and 100 Hz.

1. Introduction

The high dielectric permittivity materials exhibit potential technological applications, such as in capacitance-based components like capacitors, resonator, filters and other electronic devices [1–3]. The complex perovskite material like $\text{CaCu}_3\text{Ti}_4\text{O}_{12}$ (CCTO) has attracted much attention during the last few years due to its excellent dielectric properties. It exhibits a very high value of dielectric constant ($\epsilon' \sim 10^4$) over a wide temperature range (100–600 K) [4,5]. However, the dielectric loss ($\tan \delta$) of the CCTO ceramic is relatively high. As we know, the dielectric loss is closely related to the mechanism of the dielectric response which is explained by impedance spectroscopy measurement. Sinclair et al. demonstrated that the CCTO ceramic was electrically heterogeneous and consists of semiconducting grains and insulating grain boundaries [6]. The high dielectric constant of CCTO ceramic thus resulted from the internal barrier-layer capacitance (IBLC) effect. Undoped and doped CCTO ceramics were synthesized for the first time by the semi-wet route at a lower temperature in our laboratory and reported in different journals [7–11]. The semi-wet route in fact is a modified chemical method for the preparation of $\text{ACu}_3\text{Ti}_4\text{O}_{12}$ (A=Ca, $\text{Bi}_{2/3}$, $\text{La}_{2/3}$, $\text{Y}_{2/3}$ etc.) type of ceramics. In this method, nitrate solution of constituent ions is mixed with solid TiO_2 which is of low cost and insoluble in solvents whereas in a sol-gel method solutions of constituents ions are mixed with expensive

titanium isopropoxide [$\text{Ti}(\text{OR})_4$].

In the light of the above-mentioned literature $\text{Bi}_{2/3}\text{Cu}_3\text{Ti}_4\text{O}_{12}$ (BCTO) is an analogous to $\text{ACu}_3\text{Ti}_4\text{O}_{12}$ type ceramic having body-centered cubic structure. Which has attracted us to investigate the dielectric properties of the BCTO ceramic. As compared to CCTO, very little work has been carried out on the BCTO ceramic [12,13]. LIU et al. synthesized BCTO ceramic by conventional solid state reaction and got dielectric constant 1750 at room temperature and at 100 kHz [14]. Y.Q. Tan et al. have synthesized a series of the BCTO ceramics by conventional solid state reaction technique under different sintering temperature condition varying from 1253 to 1313 K for 10 h and observed that its microstructure was insensitive to the sintering temperature condition [15]. In the present study, BCTO ceramic was synthesized by a semi-wet route at a relatively low temperature as compared to conventional solid state ceramic method. Its microstructure, dielectric and magnetic properties were reported.

2. Experimental

2.1. Synthesis

$\text{Bi}_{2/3}\text{Cu}_3\text{Ti}_4\text{O}_{12}$ (BCTO) ceramic was synthesized by the semi-wet route. In this method chemicals bismuth nitrate, $\text{Bi}(\text{NO}_3)_3 \cdot 5\text{H}_2\text{O}$ (99.5%, Merck, India), copper nitrate, $\text{Cu}(\text{NO}_3)_2 \cdot 3\text{H}_2\text{O}$ (99.8%,

Peer review under responsibility of Chinese Materials Research Society.

* Corresponding author.

E-mail address: kdmandal.apc@itbhu.ac.in (K.D. Mandal).<http://dx.doi.org/10.1016/j.pns.2016.11.008>

Received 28 April 2016; Received in revised form 12 November 2016; Accepted 14 November 2016

Available online 10 December 2016

1002-0071/© 2017 Chinese Materials Research Society. Published by Elsevier B.V.

This is an open access article under the CC BY-NC-ND license (<http://creativecommons.org/licenses/by-nc-nd/4.0/>).

Merck, India) and titanium oxide, TiO_2 (99.9%, Merck, India) were taken in stoichiometric molar ratio. Solutions of $\text{Bi}(\text{NO}_3)_3 \cdot 5\text{H}_2\text{O}$ and $\text{Cu}(\text{NO}_3)_2 \cdot 3\text{H}_2\text{O}$ were prepared using distilled water. Both the solutions were mixed together in a beaker and solid TiO_2 was added in the solution. Calculated amount of citric acid (99.5%, Merck, India) equivalent to metal ions was dissolved in distilled water and mixed with the solution. The resulting solution was heated on a hot plate using magnetic stirrer at 343–353 K to evaporate water. The residual mass was dried at 373–393 K in hot air oven. The BCTO dry powder was calcined at 1073 K for 6 h in a muffle furnace and ground into a fine powder using a mortar and pestle. Cylindrical pellets (13.8 mmx1.00 mm) were made using a hydraulic press applying pressure of 4 tons for 1 min. The pellets were sintered at 1173 K for 8 h.

2.2. Characterization

The crystalline phase of the sintered sample was identified by X-ray diffractometer (Rigaku Miniflex 600, Japan) using $\text{CuK}\alpha$, X-ray source with a wavelength of 1.54 Å. The FTIR spectra of dry and calcined powder of BCTO were recorded by ATR-FTIR (Bruker, ALPHA model) spectrophotometer in the frequency range from 2500 cm^{-1} to 300 cm^{-1} with 4 cm^{-1} spectral resolution, using KBr pellets. The microstructures of its fractured surfaces were examined by using a scanning electron microscope (ZEISS, model EVO18 research, Germany). The elemental analysis of the sintered sample of BCTO was performed by EDX (Oxford instrument; USA) attached to SEM. The surface morphology and thickness of BCTO ceramic was examined using atomic force microscopy (NTEGRA Prima, Germany). Temperature and the field-dependent dc magnetization of BCTO ceramic was carried out by using quantum design magnetic property measurement system (MPMS-3), over a temperature range 2–300 K at a magnetic field of 7tesla. The temperature variation of field cooled (FC) and zero field cooled (ZFC) magnetization at 100 Oe applied field were carried out using SQUID VSM dc magnetometer. The dielectric data of BCTO ceramic were collected using the LCR meter (PSM 1735, Newton 4thLtd, U.K.) with the variation of frequency (100 Hz–5 MHz) and temperature (300–500 K).

3. Results and discussion

3.1. Microstructural studies

Fig. 1 shows XRD patterns of BCTO powder calcined at 873 K and 1073 K for 6 h and sintered pellet at 1173 K for 8 h. From the XRD pattern, it was observed that few secondary phases such as $\text{Bi}_4\text{Ti}_3\text{O}_{12}$, CuO and TiO_2 were present in the BCTO powder calcined at 873 K for 6 h (Fig. 1a). The single phase of BCTO was formed at 1073 K as shown in Fig. 1(b). The XRD pattern for pellet sintered at 1173 K also shows the single phase of BCTO in Fig. 1(c). XRD pattern was indexed on the bases of a body-centered cubic structure of BCTO ceramic. The lattice parameter and unit cell volume of the BCTO ceramic were determined by least squares refinement method using 'cel' software. The value of lattice parameter and unit cell volume of BCTO ceramic was found to be 7.4164 Å and 407.9160 Å^3 , respectively. The crystallite size of the BCTO ceramic was determined using the Scherrer formula [16].

$$D = k\lambda/\beta \cos \theta \quad (1)$$

where D is the crystallite size, λ is the wavelength of X-ray, k is a constant taken as 0.89, θ is the Bragg angle of the peaks and β is the full width at half maximum (FWHM) of the peak. The peak broadening due to the instrument was corrected with the data of the standard sample. The crystallite size of BCTO ceramic was calculated by using corrected value of β in the above equation. The average crystallite size of the BCTO ceramic was found to be 35.90 nm. Fig. 2 shows the FTIR spectrum of BCTO dry precursor and calcined powder at 1073 K for 6 h. Most of the citrate group disintegrates during the combustion

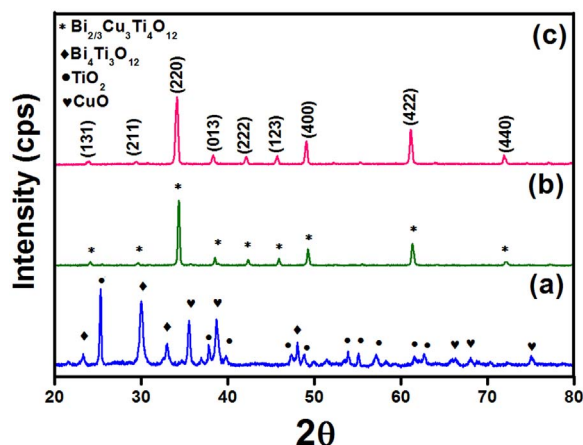


Fig. 1. XRD patterns of BCTO Ceramic calcined at (a) 873 K for 6 h (b) 1073 K for 6 h and (c) Sintered at 1173 K for 8 h.

process. The peak observed at 1637 cm^{-1} in the dry precursor and calcined powder could be assigned to the OH vibrational mode of the absorbed water molecule [17]. The nitrate band at 1384 cm^{-1} appeared for the dry precursor powder. The peaks observed at 495 cm^{-1} and 744 cm^{-1} for the calcined powder were due to bending and stretching mode of Ti-O-Ti [18]. In the low-frequency region, the peak in between 585 and 525 cm^{-1} was indicated to the Cu-O stretching vibration [19,20]. Fig. 3(a) shows microstructure of fracture surface of BCTO ceramic sintered at 1173 K for 8 h, reveals a broad distribution of spherical and faceted grains. The SEM picture showed some degree of porosity which may be due to an evolution of some significant gasses during the combustion of citrate-nitrate precursor gel [21]. The average grain size of the BCTO ceramic was found to be in the range of $0.73 \pm 0.2\text{ }\mu\text{m}$. To check the purity of synthesized pellet, the chemical composition was determined by EDX analysis. Fig. 3(b) shows the EDX spectrum of BCTO ceramic sintered at 1173 K for 8 h which confirmed the presence of Bi, Cu, Ti and O elements. Their atomic percentages were found to be 3.66, 15.10, 21.59 and 59.65 respectively. The chemical compositions of the elements were consistent with BCTO ceramic and no evidence for secondary phase formation was observed. This observation was also supported by XRD result. The AFM image of BCTO ceramic sintered at 1173 K for 8 h was examined. Fig. 4(a) shows the surface morphology of grains and grain boundary for a two-dimensional image of BCTO ceramic. The AFM image of BCTO ceramic exhibits compact structure with granular morphology, buffer layer, plates like grains and clear grain boundary [22]. Fig. 4(b) shows three-

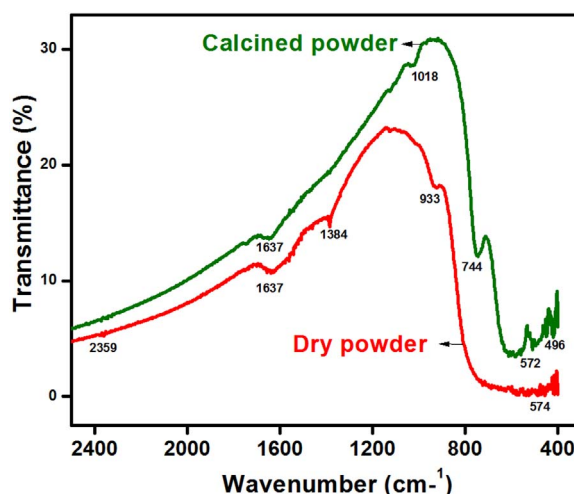


Fig. 2. FTIR spectra for the BCTO ceramic (a) Dry powder (b) calcined at 1073 K for 6 h.

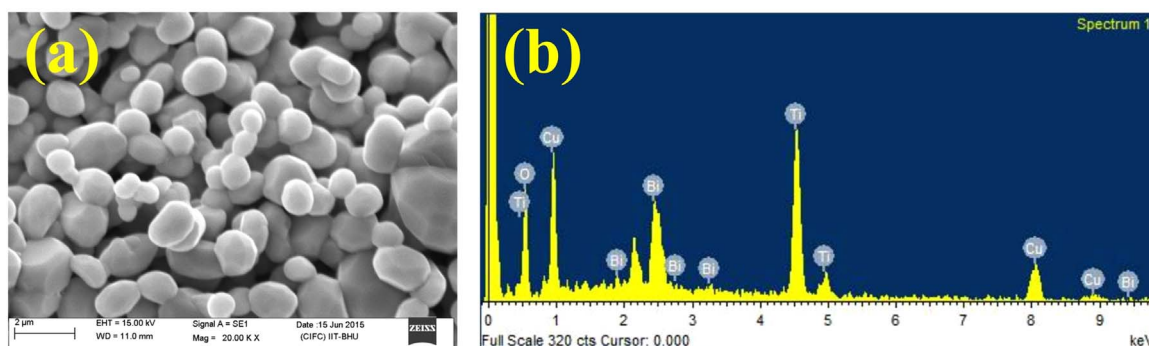


Fig. 3. (a). SEM morphology of BCTO ceramic sintered at 1173 K for 8 h and (b) the corresponding EDX spectra of BCTO ceramic.

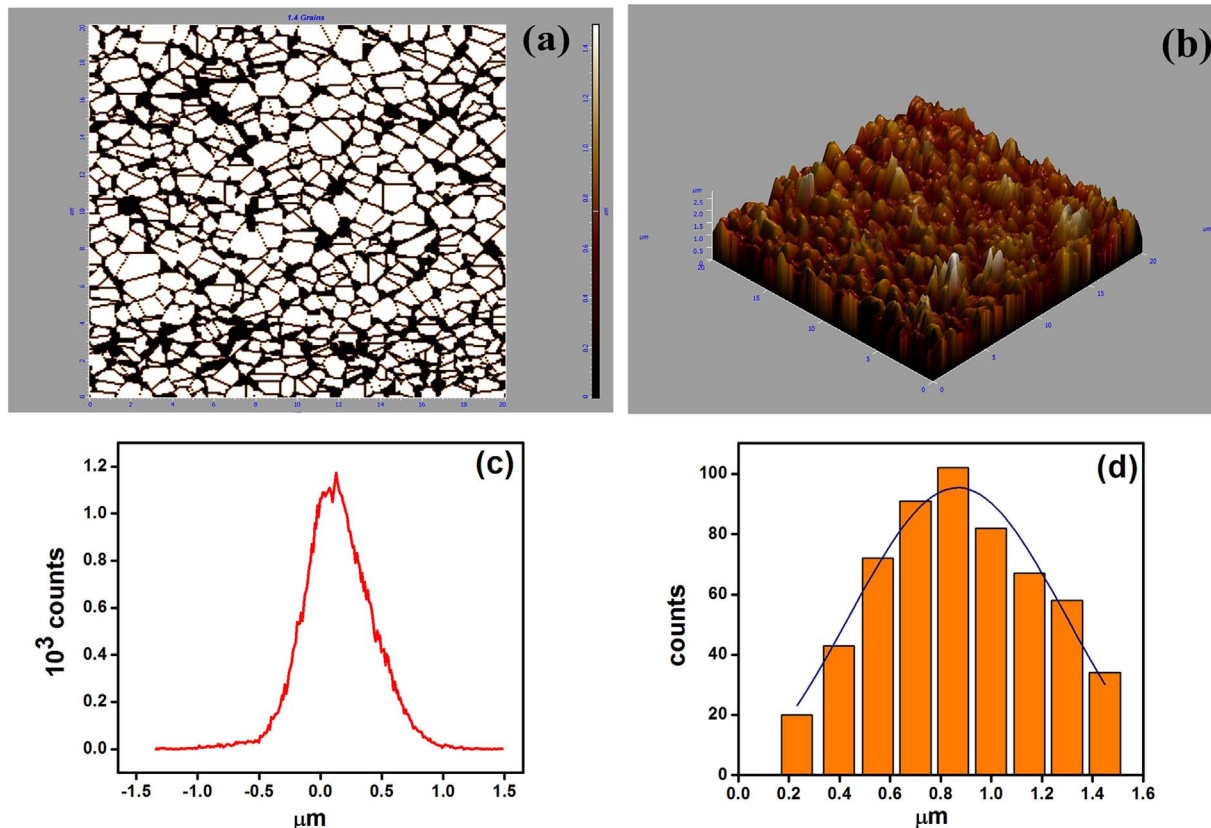


Fig. 4. AFM images of BCTO Ceramic sintered at 1173 K for 8 h (a) two-dimensional image showing grains and grain boundaries (b) three-dimensional image (c) Histogram of three-dimensional particle roughness and (d) Particle size distribution curve.

dimensional AFM image of BCTO ceramic which exhibits the maximum peak height of the grain to be 0.420 μm within the scan area 20 μm × 25 μm. Fig. 4(c) shows the three-dimensional surface roughness of BCTO ceramic. The average and root mean square roughness were found to be 0.220 μm and 0.285 μm, respectively. The AFM analysis revealed the presence of the particles with the wider size distribution in the BCTO ceramic. The average grain size estimated by two-dimensional AFM image was found to be 0.615 μm out of 625 grains as shown in the histogram Fig. 4(d) which was also supported by SEM analysis.

3.2. Magnetic measurements

The temperature dependent magnetization studies were carried out during cooling and heating mode for BCTO ceramic over a temperature range 2–300 K at fixed applied field of 100 Oe. The variation of zero field cooled (M^{ZFC}) and field cooled (M^{FC}) magnetizations were explained as a function of temperature for BCTO ceramic which is

shown in Fig. 5(a). It was observed from the figure that the magnetization behavior for the BCTO ceramic the M^{ZFC} values at low temperatures was always lower than M^{FC} values, but at high temperatures, the two curves merge together [23,24]. The M^{ZFC} curve follows the same path as the M^{FC} . The bifurcation in magnetization in M^{ZFC} and M^{FC} shows a peak at 27 K. The peak of M^{FC} and M^{ZFC} curves were observed at the same temperature but with different magnetic moments. M^{ZFC} and M^{FC} show the peak at 27 K and the values of magnetic moment were found to be 0.00348 emu/g and 0.00354 emu/g respectively. The extrapolation of the linear part intercept at 125 K on the temperature axis, which is known as the Curie temperature (T_c) [25]. Further, magnetic moment decreases with decrease in temperature in both the curves. The Blocking temperature for the BCTO ceramic was observed at 25 K (Fig. 5a) which increases with a magnetic moment at the constant applied field (100 Oe). Fig. 5(b) exhibits the variation of magnetic moment with a magnetic field. The magnetic moment increases linearly with the magnetic field at room temperature (300 K) which shows the paramagnetic phase. In the BCTO ceramic,

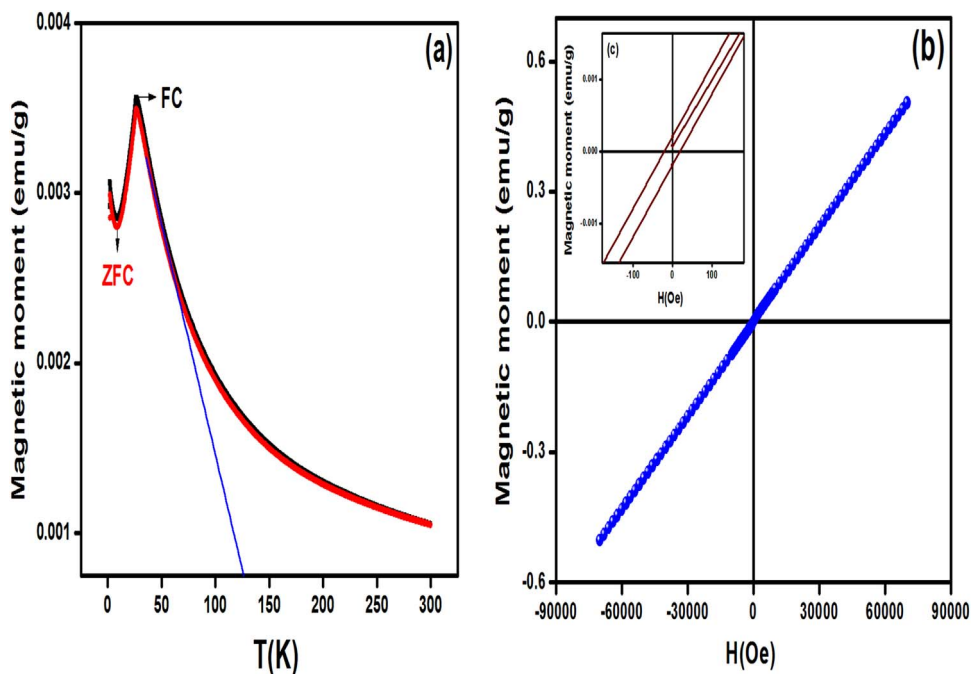


Fig. 5. (a) Temperature-dependent zero field cooled (ZFC) and field cooled (FC) magnetization measured at $H=100$ Oe and (b) magnetization versus applied field at 300 K for the BCTO ceramic.

the non-saturated hysteresis loop was also observed between the magnetic moment $-0.4-0.4$ emu/g. The magnetization increases linearly from a low field to high magnetic field. From the inset a non-saturated hysteresis loop was obtained within the field -100 Oe to 100 Oe. It exhibits a coercivity of ~ 21.96 Oe. The appearance of such non-saturated hysteresis loop from -0.4 to 0.4 Oe and its disappearance below -0.4 Oe distinctly suggest the transformation from paramagnetic phase to superparamagnetic phase [26].

3.3. Dielectric studies

Fig. 6(a) shows the variation of dielectric constant (ϵ') and dielectric loss ($\tan\delta$) of BCTO ceramic with temperature at few selected frequencies. The dielectric constant of BCTO ceramic shows temperature independent behavior from 400 K to 500 K at all measured frequencies (100 Hz, 1 kHz, 10 kHz and 100 kHz). Below 400 K, dielectric broad peaks were observed at around 340 K for all measured frequencies. It is also observed that dielectric constant decreases with increasing frequency. The dielectric constant of BCTO ceramic was found to be 2.9×10^4 , 3.6×10^3 , 8.5×10^2 , 3.5×10^2 at 100 Hz, 1 kHz, 10 kHz and 100 kHz at 323 K, respectively. Fig. 6(b) shows dielectric loss peaks with temperature at 340 K and 408 K with all measured frequencies. The minimum values of $\tan \delta$ of BCTO ceramic were found to be 0.598, 0.251, 0.116 and 0.106 at 100 Hz, 1 kHz, 10 kHz and 100 kHz respectively at 423 K. The broad peaks observed at 340 K for dielectric constant and dielectric loss are likely to be caused by oxygen vacancy and not by relaxation process. The oxygen vacancy was created in the BCTO ceramic during the sintering process [27]. Fig. 7(a) shows the variation of dielectric constant (ϵ') and dielectric loss ($\tan \delta$) with frequency at few selected temperatures. It is observed from the figure that dielectric constant decreases with increasing frequency rapidly up to 1 kHz and after that it remains constant at all measured temperatures. Fig. 7(b) shows the dielectric relaxation peaks below 10 kHz at all measured temperatures and after that, its dielectric loss remains constant at high temperature. The decrease in dielectric constant with frequency may be exhibited by space charge polarization [28]. It is believed that defects such as oxygen vacancies inherently present during sintering in these ceramic oxide materials due to space charges

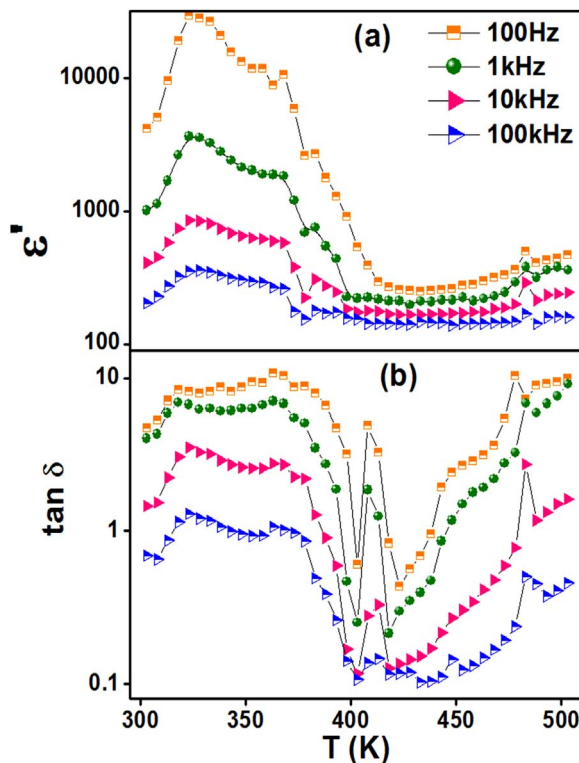


Fig. 6. Plot of (a) Dielectric constant and (b) $\tan \delta$ as a function of temperature for BCTO ceramic sintered at 1173 K for 8 h.

whose polarization can respond to the external electric field [29]. At low frequencies, these charges have enough time to move longer distances in the material, creating a more electronic polarization. Therefore, a high value of dielectric constant is observed. At higher frequency, the space charge no longer follows the field leading to lower values of dielectric constant.

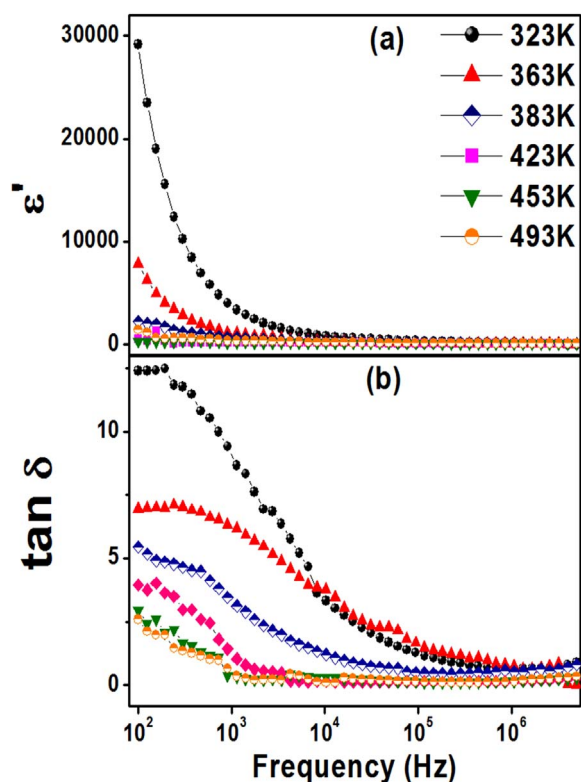


Fig. 7. Plot of (a) Dielectric constant and (b) $\tan \delta$ as a function of frequency for BCTO ceramic sintered at 1173 K for 8 h.

4. Conclusions

- In this study $\text{Bi}_{2/3}\text{Cu}_3\text{Ti}_4\text{O}_{12}$ (BCTO) ceramic was synthesized by semi wet route at low temperature and single phase formation confirmed by XRD.
- The O-H, Ti-O and Cu-O band stretching frequency were confirmed by FTIR in the BCTO ceramic calcined at 1073 K.
- The SEM study of BCTO ceramic sintered at 1173 K for 8 h exhibited average grain size $0.73 \pm 0.2 \mu\text{m}$ and fine grain boundary which was also substantiated by AFM study. EDX spectrum shows the presence of Bi, Cu, Ti and O elements and the atomic percentage are inconsistent with stoichiometric of BCTO ceramic.
- The magnetic studied of BCTO ceramic shows paramagnetic to the super paramagnetic phase transition.
- The dielectric constant (ϵ') of BCTO ceramic was found to be 2.9×10^4 at 100 Hz. The high Dielectric constant was due to IBLC

effect presence in the ceramic.

Acknowledgments

Authors are thankful to the Central Instrument Facility Centre (CIFC) IIT BHU, Varanasi for SEM, EDX, and AFM facilities and one of the authors Pooja Gautam is grateful to IIT(BHU) (Grant No.13051009) for financial support as teaching assistantship.

References

- [1] M.A. Subramanian, D. Li, N. Duan, B.A. Reisner, A.W. Sleight, *J. Solid State Chem.* 151 (2000) 323.
- [2] B.C. Sutar, P.R. Das, R.N.P. Choudhary, *Adv. Mat. Lett.* 5 (3) (2014) 131–137.
- [3] G.H. Haertling, *J. Am. Ceram. Soc.* 82 (1999) 797–818.
- [4] S. Ezhilvalavan, T.Y. Tseng, *Mater. Chem. Phys.* 65 (2000) 227–248.
- [5] L.C. Kretly, A.F.L. Almeida, R.S.D. Oliveira, J.M. Sasaki, A.S.B. Sombra, *Micro Opt. Technol. Lett.* 39 (2003) 145–150.
- [6] D.C. Sinclair, T.B. Adams, F.D. Morrison, A.R. West, *J. Appl. Phys. Lett.* 80 (2002) 2153–2155.
- [7] L. Singh, A.K. Rai, U.S. Rai, K.D. Mandal, *Electron. Mater. Lett.* 9 (2013) 107–113.
- [8] K.D. Mandal, A.K. Rai, D. Kumar, O. Prakash, *Mater. Chem. Phys.* 122 (2010) 217–223.
- [9] K.D. Mandal, A.K. Rai, D. Kumar, O. Prakash, *J. Alloy. Compd.* 491 (2010) 507–512.
- [10] K.D. Mandal, A.K. Rai, D. Kumar, O. Prakash, *J. Phys. Chem. Solids* 70 (2009) 834–839.
- [11] K.D. Mandal, A.K. Rai, D. Kumar, O. Prakash, *J. Alloy. Compd.* 478 (2009) 771–776.
- [12] L. Singh, I.W. Kim, B.C. Sin, Sk Woo, S.H. Hyun, K.D. Mandal, Y. Lee, *Powder Technol.* 280 (2015) 256–265.
- [13] J. Liu, C.G. Duan, W.G. Yin, W.N. Mei, R.W. Smith, J.R. Hardy, *J. Appl. Phys.* 98 (2005) 093703.
- [14] J. Liu, C.G. Duan, W.G. Yin, W.N. Mei, R.W. Smith, J.R. Hardy, *Phys. Rev. B* 70 (2004) 144106.
- [15] Y.Q. Tan, J.L. Zhang, W.T. Hao, G. Chen, W.B. Su, C.L. Wang, *Mater. Chem. Phys.* 124 (2010) 1100–1104.
- [16] L. Singh, U.S. Rai, K.D. Mandal, *Nanomater. Nanotechnol.* 1 (2011) 59–66.
- [17] A.R. Ocwelwang, L. Tichagwa, *Int. J. Adv. Res. Chem. Sci.* 1 (2014) 28–37.
- [18] R.D. Sharmila, R. Venkatesh, R. Sivaraj, *Int. J. Innov. Res. Sci. Eng. Technol.* 3 (1) (2014) 5206–15211.
- [19] B.V. Rao, A.D.P. Rao, V.R. Reddy, *Int. J. Innov. Res. Sci. Eng. Technol.* 2 (7) (2013) 768–7779.
- [20] H. Tachikawa, T. Iyama, T. Hamabayashi, *J. Theor. CH* 2 (1997) 263–267.
- [21] L.D. Conceicao, A.M. Silva, N.F.P. Ribeiro, M.M.V.M. Souza, *Mater. Res. Bull.* 46 (2011) 308–314.
- [22] R.K. Nimat, R.S. Joshi, S.H. Pawar, *J. Alloy. Compd.* 466 (2008) 341–351.
- [23] C. Rath, S. Anand, R.P. Das, K.K. Sahu, S.D. Kulkarni, S.K. Date, N.C. Mishra, *J. Appl. Phys.* 91 (2002) 4.
- [24] C. Rath, K.K. Sahu, S. Anand, S.K. Date, N.C. Mishra, R.P. Das, *J. Magn. Magn. Mater.* 202 (1999) 77–84.
- [25] C. Rath, P. Mohanty, *J. Superd. Nov. Magn.* 24 (2011) 629–633.
- [26] L. Kumar, P. Mohanty, T. Shripathi, C. Rath, *Nanosci. Nanotechnol. Lett.* 1 (2009) 199–203.
- [27] C.C. Wang, L.W. Zhang, *Phys. Rev. B* 74 (2006) (024106-4).
- [28] C.G. Koops, *Phys. Rev.* 83 (1951) 121.
- [29] K.W. Wagner, *Ann. Phys.* 40 (1913) 817.